

Continued Protein Synthesis at Low [ATP] and [GTP] Enables Cell Adaptation during Energy Limitation[∇]

Michael C. Jewett,^{1†} Mark L. Miller,¹ Yvonne Chen,¹ and James R. Swartz^{1,2*}

Department of Chemical Engineering¹ and Department of Bioengineering,² Stanford University, Stanford, California 94305

Received 22 June 2008/Accepted 9 November 2008

One of biology's critical ironies is the need to adapt to periods of energy limitation by using the energy-intensive process of protein synthesis. Although previous work has identified the individual energy-requiring steps in protein synthesis, we still lack an understanding of the dependence of protein biosynthesis rates on [ATP] and [GTP]. Here, we used an integrated *Escherichia coli* cell-free platform that mimics the intracellular, energy-limited environment to show that protein synthesis rates are governed by simple Michaelis-Menten dependence on [ATP] and [GTP] (K_m^{ATP} , $27 \pm 4 \mu\text{M}$; K_m^{GTP} , $14 \pm 2 \mu\text{M}$). Although the system-level GTP affinity agrees well with the individual affinities of the GTP-dependent translation factors, the system-level K_m^{ATP} is unexpectedly low. Especially under starvation conditions, when energy sources are limited, cells need to replace catalysts that become inactive and to produce new catalysts in order to effectively adapt. Our results show how this crucial survival priority for synthesizing new proteins can be enforced after rapidly growing cells encounter energy limitation. A diminished energy supply can be rationed based on the relative ATP and GTP affinities, and, since these affinities for protein synthesis are high, the cells can adapt with substantial changes in protein composition. Furthermore, our work suggests that characterization of individual enzymes may not always predict the performance of multicomponent systems with complex interdependencies. We anticipate that cell-free studies in which complex metabolic systems are activated will be valuable tools for elucidating the behavior of such systems.

Arguably, new protein synthesis is most crucial when energy supplies are limited and the cell must adjust its catalytic capabilities to cope with this challenge. Yet, paradoxically, due to the entropic demands for accurate transcription and translation, the metabolic system for protein synthesis is typically the most energy-demanding process in most organisms (Fig. 1). It has been shown, for example, that protein synthesis consumes approximately two-thirds of the total energy produced by a rapidly growing *Escherichia coli* cell (30). Consequently, much effort has been focused on understanding the mechanisms of ATP and GTP usage during protein synthesis.

Previous work has established the individual energy-requiring steps for the metabolic system for protein synthesis (Fig. 1). These steps include recycling nucleotides for mRNA synthesis (44), charging aminoacyl-tRNAs (44), and regenerating GTP to energize the translation factors required for polypeptide synthesis (initiation factor 2 [IF-2], elongation factor Tu [EF-Tu], elongation factor G [EF-G], and ribosome release factor 3 [RF-3]) (53). The GTP-GDP cycle of EF-Tu, for example, plays a key role in tRNA selection and kinetic proofreading (4, 18). In addition to transcription and translation, the DEAD box RNA helicase, which is required for unwinding mRNA secondary structure, is ATP dependent (36), as are several chaperones (14, 16). Relative to the energy required for addition of one amino acid to a growing polypeptide chain (four

ATP molecules), the energy necessary for mRNA synthesis and degradation is negligible since each message is used many times (27).

While a broad range of ATP and GTP affinities have been measured for individual catalytic steps using in vitro enzyme methods (1, 15, 17, 25, 54), we still lack an understanding of the dependence of protein synthesis rate on [ATP] and [GTP] from a system-level perspective. Although the affinities of the translation factors for GTP, for example, are high ($\leq 10 \mu\text{M}$) (1, 15, 25, 54), the affinities of the aminoacyl-tRNA synthetases for ATP that have been determined are much lower (100 to 700 μM) (17). Thus, we are left with the critical question of how overall systemic rates respond to limiting [ATP] and [GTP]. This study was designed to help us explore the hypothesis that ATP rationing among energy-dependent metabolic processes (based on their relative affinities for nucleoside triphosphates) still allows the substantial protein synthesis required for the organism to remodel itself in order to survive. Moreover, evaluation of the affinities is required for development of authentic in silico models that seek to describe integrated cellular physiology (42).

Measuring the rate of protein synthesis as a function of [ATP] and [GTP] in vivo is extremely difficult because of our inability to precisely control and measure intracellular concentrations of ATP and GTP. During exponential growth, [ATP] and [GTP] are relatively constant (approximately 3 mM and 900 μM , respectively) over a wide range of growth rates (31, 35, 40). During energy-limited growth, ATP and GTP concentrations undoubtedly become very low relative to the rates of metabolic flux. It then is very difficult to obtain representative samples, and, with current technology, it is essentially impossible to precisely control very low intracellular ATP and GTP

* Corresponding author. Mailing address: Department of Chemical Engineering, Stanford University, Stauffer III, Rm. 113, Stanford, CA 94305-5025. Phone: (650) 723-5398. Fax: (650) 725-0555. E-mail: jswartz@stanford.edu.

† Present address: Department of Genetics, Harvard Medical School, MA 02115.

[∇] Published ahead of print on 21 November 2008.

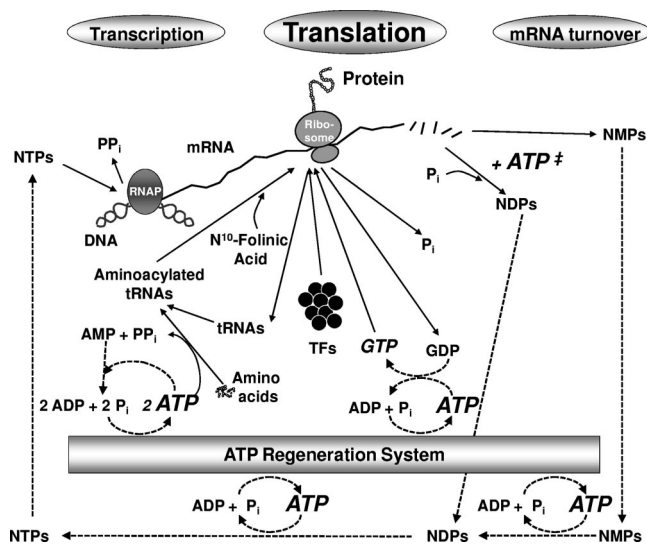


FIG. 1. Metabolic system for protein synthesis: global view of the protein synthesis system comprising transcription, translation, and mRNA turnover. ATP is required for recycling nucleotides used in mRNA synthesis, for charging aminoacyl-tRNAs, for regenerating GTP for the translation factors involved in peptide bond formation, for ATP-dependent RNA (DEAD box) helicase activity (indicated by a double dagger), and for several chaperones. GTP is required for translation initiation and for elongation and termination. In our system, ATP is regenerated from central metabolism coupled to membrane-dependent respiration (21). TFs, translation factors; P_i, phosphate; PP_i, pyrophosphate; NTPs, nucleoside triphosphates; NDPs, nucleoside diphosphates; NMPs, nucleoside monophosphates; RNAP, RNA polymerase.

concentrations in vivo. Beyond challenges related to controlling specific ATP and GTP concentrations, quenching in vivo metabolism and extracting intracellular metabolites without altering concentrations are technical hurdles. Recently developed extraction strategies coupled with quantitative mass spectrometry are, however, beginning to enable workers to obtain more consistent results (19, 32).

To measure the dependence of the protein synthesis rate on [ATP] and [GTP], we used an in vitro cell-free system derived from *E. coli* extracts. Cell-free systems provide the opportunity to directly monitor, add, and remove components with much greater ease and accuracy than can be done with in vivo systems. In addition, they have the potential to reproduce much of the complexity of in vivo metabolism without the threat that the catalytic system will be altered by continued synthesis of system components.

A key challenge in studying in vivo physiology with in vitro systems is mimicking the cellular environment. The cell-free protein synthesis platform that we used, called the Cytomim system, was developed to address this challenge (22). The physicochemical environment of this system attempts to reconstruct the natural balance of ionic components in living cells (22). Equally important, the Cytomim system has been shown to coactivate multiple complex biochemical networks using a single integrated platform, including central catabolism, oxidative phosphorylation, transcription, translation, and protein folding (21). Radioactive glucose tracing showed that glycolysis is active (6), and L-[U-¹⁴C]glutamate metabolic studies dem-

onstrated that the tricarboxylic acid cycle and glutamate catabolism are active (21). Dramatic decreases in protein synthesis upon addition of biochemical inhibitors of the electron transport chain and the F₁F₀ ATPase, as well as membrane gradient uncouplers, provided evidence of activation of oxidative phosphorylation from inverted membrane vesicles (21). Furthermore, the protein production rates are the expected rates for a second-order kinetic system that has been diluted approximately 20-fold relative to cytoplasmic concentrations (M. C. Jewett and J. R. Swartz, unpublished data). In addition, the specific oxygen uptake rate is about one-half the rate observed using intact *E. coli* cells (based on lipid measurements to determine the membrane content of the extracts) (21). Finally, the overall catalytic system is capable of supporting robust protein synthesis ($\sim 400 \mu\text{g protein ml}^{-1} \text{ h}^{-1}$) such that each ribosome (translating in polysomes with up to seven or eight ribosomes per message) produces, on average, about 20 to 30 new proteins during the course of the reaction (47).

Here we used the Cytomim system to investigate the dependence of the protein synthesis rate on [ATP] and [GTP] in an integrated multicomponent network. We found Michaelis-Menten relationships with an unexpectedly high affinity for ATP. The GTP affinity, on the other hand, agrees well with previously measured affinities for the individual GTP-dependent components of the translation system, providing confidence in our data. Although the Cytomim platform closely mimics intracellular functions, two points must be raised. First, growth of the extract source cells occurs under energy-rich conditions. Second, the ribosome and cofactor concentrations are ~ 20 -fold lower in the cell-free system than in cells at the maximum growth rate. Since such concentrations (i.e., a dilute ribosome pool) occur when cells enter energy-limited stationary phase (5), the conclusions drawn from our results can be conservatively applied to cells that are shifted from rapid growth to slow growth, but they may also be more general. We suggest that the unexpectedly high ATP affinity allows cells to preferentially channel energy resources to protein synthesis in order to implement survival mechanisms requiring substantial cellular adaptation. This study also revealed the significant contributions that carefully designed and integrated cell-free systems can make to the study of cellular physiology.

MATERIALS AND METHODS

S30 extract preparation. S30 cell extract was prepared from *E. coli* strain KC1, a derivative of *E. coli* K-12 (7). Cells were grown in a 10-liter fermentor (Braun C-10-2 No.153-10L fermentor; B. Braun Biotech Inc., Allentown, PA) to an optical density (A_{600}) of 3.3 on defined medium (55). Cell extract was prepared as previously described (46).

Cell-free protein synthesis and product determination. Semicontinuous cell-free protein synthesis reactions (26) using 250- μl mixtures were performed in Slide-A-Lyzer minidialysis units (Pierce, Rockford, IL) with a 7,000-molecular-weight-cutoff regenerated cellulose dialysis membrane (Fig. 2). The reaction units were partially immersed in a 2-ml stabilization bath. The stabilization bath was in a 10-ml glass beaker suspended in a water bath. The water bath was used to maintain an internal reaction temperature of $37 \pm 1^\circ\text{C}$. Both the contents of the reaction chamber and the reagent bath were stirred at 125 rpm.

Cell-free protein synthesis reactions were carried out as previously described (22). The standard reaction mixture for the internal reaction solution contained the following components: 0.85 mM UTP, 0.85 mM CTP, 34 $\mu\text{g/ml}$ folinic acid, 170 $\mu\text{g/ml}$ *E. coli* tRNA mixture (Roche, Indianapolis, IN), 13.3 $\mu\text{g/ml}$ pk7CAT plasmid (encoding the chloramphenicol acetyltransferase [CAT] gene behind the T7 promoter [27]), 100 $\mu\text{g/ml}$ T7 RNA polymerase, 5 μM L-[U-¹⁴C]leucine (11.8GBq/mmol; 318 mCi/mmol; Amersham Pharmacia, Uppsala, Sweden), 2

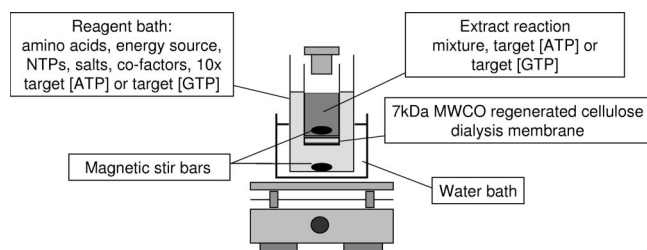


FIG. 2. Experimental setup for maintaining constant [ATP] or [GTP]. The cell-free reaction mixture was separated from a stabilization bath containing all of the reagents in the reaction chamber except the pk7CAT plasmid, T7 RNA polymerase, and cell extract. In addition, to facilitate diffusion into the reaction chamber, the ATP concentrations in the reagent bath were greater than those in the reaction chamber. A water bath was used to maintain an internal reaction temperature of 37°C. NTPs, nucleoside triphosphates; MWCO, molecular weight cutoff.

mM each of 20 unlabeled amino acids, 0.33 mM NAD, 0.26 mM coenzyme A, 33 mM sodium pyruvate, 130 mM potassium glutamate, 10 mM ammonium glutamate, 1.5 mM spermidine, 1 mM putrescine, 4 mM sodium oxalate, and 0.24 volume of S30 extract. Each reaction mixture contained an additional approximately 3.3 mM magnesium, 14.4 mM potassium, 2.4 mM Tris, and 23.5 mM acetate originating from the cell extract. Magnesium glutamate was added to obtain the total magnesium concentrations indicated in the Results. T7 RNA polymerase was prepared as previously described (46). For the constant-[ATP] experiments, the initial GTP concentration was 1 mM and at all times the GTP concentration was maintained at levels well above the system K_m^{GTP} . For each ATP concentration, it was necessary to optimize the Mg^{2+} concentration to obtain maximal protein production rates. For the constant-[GTP] experiments, the ATP concentration was maintained at 1.0 ± 0.1 mM, and the magnesium glutamate concentration was 18 mM.

The stabilization bath contained the same concentrations of reagents as the reaction chamber except that the pk7CAT plasmid, T7 RNA polymerase, and cell extract were not present. In addition, the [ATP] and [GTP] in the stabilization bath were empirically titrated to ensure that the [ATP] and [GTP] in the reaction mixture were constant. Potassium hydroxide was added to the reagent bath so that the pH equaled that of the cell-free reaction mixture (pH 6.8).

Before protein synthesis was initiated, the support solution was warmed to 37°C for 10 min in the experimental apparatus. Next, the cell extract and a mixture of the reagents necessary for protein synthesis were incubated separately at 37°C for 5 min. The two solutions were then mixed to start protein biosynthesis and were immediately added to the reaction chamber. Samples were taken at 5-min intervals to measure CAT accumulation using [^{14}C]leucine incorporation and to monitor nucleotide concentrations. Control transcription and translation reactions without plasmid DNA were used to assess the apparent background protein production levels, which were subtracted from sample data.

Total amounts of synthesized CAT were determined using a liquid scintillation counter to measure the incorporation of [^{14}C]leucine into trichloroacetic acid (TCA)-precipitable polypeptides (46). To determine the amount of protein produced, we divided the fraction of incorporated leucine by the number of leucine residues in CAT (13 residues) and multiplied by the total concentration of leucine in the reaction mixture (2,000 μ M). The resulting value was converted from a molar value to a gram value using the molecular weight of CAT. To determine the fraction of incorporated leucine, each protein synthesis sample was divided into two parts. One part was TCA precipitated, and the other was not. The fraction of incorporated leucine was obtained by dividing the cpm of the precipitated sample by the cpm of the nonprecipitated sample. To illustrate, the following is a sample calculation if the TCA-precipitated count was 950 cpm, the nonprecipitated count was 9,996 cpm, and the background count from an experiment without plasmid DNA was 73 cpm (Table 1): $\{(950 \text{ cpm} - 73 \text{ cpm})/9,996 \text{ cpm}\} \times 2,000 \mu\text{M} \times 25,000 \mu\text{g}/\mu\text{mol}/(13 \times 1,000 \text{ ml/liter}) = 337 \mu\text{g CAT/ml}$.

Previously, we showed that approximately 100% of the CAT produced during the initial protein synthesis period (the first hour) is active (21, 22). Thus, in the experiments performed here, the TCA-precipitable counts were a good indication of the active protein concentration.

Measurement of ATP and GTP concentrations. [ATP] and [GTP] were quantified using high-performance liquid chromatography (HPLC) peak integration

(23). A sample of a cell-free reaction mixture was added to an equal volume of 5% TCA at 4°C. TCA-precipitated samples were centrifuged at $12,000 \times g$ for 15 min at 4°C. The supernatant was collected, and 20- μ l samples were applied directly to a Vydac 302IC4.6 ion chromatography column (Hesperia, CA) for separation and analysis. ATP and GTP concentrations lower than 0.1 mM were below the sensitivity of the detector. For ATP concentrations lower than 0.1 mM and to verify all HPLC concentration measurements, we also used a firefly luciferase assay (27). Samples used in the luciferase assay were adjusted to pH 7.8 before their activity was tested. The ATP concentrations determined by the HPLC and luciferase methods were equivalent. GTP concentrations less than 0.1 mM were estimated to be constant at the [GTP] actually added to the system. For energy charge (EC) calculations, [ADP] and [AMP] were determined using the HPLC method described above.

RESULTS

Protein synthesis rate as a function of [ATP]. The objective of this study was to determine the rate of protein synthesis as a function of [ATP]. To achieve this objective, we needed to (i) provide a chemical reaction environment that was as similar as possible to that inside a living bacterium, (ii) avoid limiting the multisubstrate protein synthesis system reaction (transcription and translation) by any other component, and (iii) measure protein synthesis rates at different ATP concentrations while confirming that [ATP] was indeed constant.

To mimic intracellular physiology *in vitro*, we used the Cyto-mim combined transcription-translation system derived from crude extract of *E. coli* strain A19 Δ speA Δ tnaA Δ sdaA Δ sdaB Δ tonA Δ endAmet $^{+}$ (7). Deletion of the *speA* gene, which codes for arginine decarboxylase, prevents arginine degradation. Deletion of the *tnaA* gene, which encodes for tryptophanase, eliminates tryptophan degradation. Deletion of two serine deaminases, the products of the *sdaA* and *sdaB* genes, stabilizes serine. Deletion of the *tonA* gene, encoding the outer membrane protein TonA (or FhuA), blocks the adsorption of T5 bacteriophages to eliminate infection during cell growth for extract preparation. Deletion of the *endA* gene, which codes for DNA-specific endonuclease I, stabilizes the DNA. Finally, the methionine auxotrophy of the A19 strain was also reverted to methionine prototrophy. Crude cell extract (specifically, the S30 fraction) was prepared from *E. coli* cells grown in a well-controlled fermentor and harvested during mid-exponential growth at an A_{600} of 3.3 (46). A crude extract system was chosen because it provided all of the components necessary for transcription, translation, protein folding, and energy metabolism (e.g., ribosomes, aminoacyl-tRNA synthe-

TABLE 1. Sample radioactivity data used to evaluate the protein produced over time at three ATP concentrations

Time (h)	Radioactivity (cpm) ^a			
	Background (no plasmid)	1.2 mM ATP	0.11 mM ATP	0.015 mM ATP
0	79	56	79	62
0.17	62	247	139	106
0.25	67	396	200	140
0.33	62	504	272	173
0.42	79	580	308	197
0.5	68	658	398	214
0.58	58	752	444	241
0.67	61	854	518	285
0.75	73	950	605	319

^a Counts retained after TCA precipitation and sample washing. The average nonprecipitated value was $9,996 \pm 283$ cpm.

tases, translation factors, nucleotide-recycling enzymes, catalysts involved in metabolic pathways, inverted inner membrane vesicles, chaperones, etc.). The Cytomim system has been carefully optimized for maximal protein synthesis rates ($\sim 400 \mu\text{g/ml/h}$) in a chemical environment that closely mimics the *E. coli* cytoplasm and activates integrated metabolic networks (21, 22).

To ensure that the multisubstrate protein synthesis reaction was not limited by substrates other than ATP, cell-free protein synthesis reactions were performed in a semicontinuous reaction chamber (Fig. 2). A large volume of support reagents (containing extra substrates, such as amino acids and nucleoside triphosphates) was separated from the reaction mixture by a dialysis membrane. This served two purposes. First, substrate concentrations were stabilized by diffusion from the surrounding solution into the reaction chamber. Second, by-products that might otherwise have become inhibitory could diffuse away from the reaction mixture into the support solution. For example, ADP and AMP were removed to maintain a stable and high EC.

Using this cell-free platform, we determined the rate of CAT expression as a function of [ATP]. CAT was used to evaluate the system while it was engaged in synthesizing a full-length protein rather than shorter polypeptides. Production rates were assessed by quantifying the incorporation of [^{14}C]leucine into TCA-precipitable protein, and ATP and GTP concentrations were monitored by HPLC and an enzymatic assay. Autoradiograms confirmed that only CAT was produced since the T7 RNA polymerase limited transcription to the T7 promoter on the plasmid added to the reaction mixture.

Preliminary experiments provided two critical insights. First, to maintain a constant [ATP] in the reaction chamber, a concentration gradient between the support solution and the protein synthesis reaction chamber was required. Although the Cytomim system is capable of robust ATP generation (21), the reaction configuration limited oxygen transfer into the reaction mixture, thereby limiting intrinsic ATP synthesis from oxidative phosphorylation. Second, to obtain maximal protein production rates, it was necessary to titrate total Mg^{2+} concentrations for each ATP concentration. Magnesium is important for many processes in the metabolic system (e.g., energy transfer by nucleotide kinases [44], as well as aminoacyl-tRNA synthetase activity [17, 48]), and the ATP concentration affects the concentration of unassociated magnesium {reported log stability constant ($[\text{MgATP}]/[\text{Mg}][\text{ATP}]$), 4.22 (11)}. The optimal Mg^{2+} concentration for each [ATP] is shown in Fig. 3. The experimentally determined optima, ranging from 12 to 18 mM, are higher than those typically used for in vitro translation systems composed of purified components ($\sim 5 \text{ mM}$) (20, 34). This discrepancy likely resulted from our efforts to mimic the intracellular physicochemical environment (22). Glutamate, for example, is present at concentrations between ~ 50 and 350 mM in vivo depending on the stress level of the cell (12, 38, 39). While glutamate is not generally used in purified translation systems (20, 34) or purified enzyme systems (3), the concentration of glutamate in the Cytomim system is $\sim 150 \text{ mM}$ (22). Given that the reported log stability constant for $[\text{MgGlu}^-]/[\text{Mg}][\text{Glu}]$ is 1.9 (11), it seems reasonable that 150 mM glutamate would have a strong buffering effect on the concentration of free Mg^{2+} and would therefore impact the observed optimum for total $[\text{Mg}^{2+}]$. This is consistent with

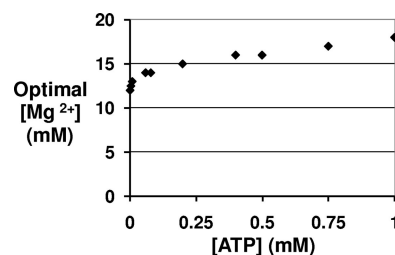


FIG. 3. Optimum total magnesium concentrations for constant-[ATP] cell-free protein synthesis experiments for the range of ATP concentrations investigated. ATP concentrations were measured inside the reactor.

data obtained with the PURE in vitro translation system, which recently showed that the optimum magnesium concentration was 13 mM when 100 mM glutamate was used (41).

After preliminary experiments determined the optimum $[\text{Mg}^{2+}]$ and the means to maintain a constant [ATP], protein production rates were quantified by performing linear regression analysis of the production profiles (typically between about 10 and 45 min after initiation of the reaction) (Table 1). Representative protein production rates and ATP concentration profiles are shown in Fig. 4A and 4B. These experiments revealed a Michaelis-Menten dependence of the protein synthesis rate on the ATP concentration (Fig. 4C), which is shown by the Lineweaver-Burk plot in Fig. 4D. The Michaelis-Menten constants obtained by using a least-squares fit to the data in Fig. 4C are as follows: K_m^{ATP} , $27 \pm 4 \mu\text{M}$; and V_{max} , $41 \pm 1 \mu\text{g CAT/h/mg } E. coli \text{ protein}$ (each reaction mixture contained $\sim 10 \text{ mg/ml}$ of protein from the cell extract).

The linearity of the CAT production rates and the explicit dependence on ATP concentration suggest that the system was not limited for other substrates. Measurements also indicated that the EC in our experiments was consistent with maximal protein synthesis rates (8, 52). EC, which was defined by Atkinson as the overall status of energy availability in the system, $([\text{ATP}] + 0.5[\text{ADP}])/([\text{ATP}] + [\text{ADP}] + [\text{AMP}])$, has been hypothesized to be an important regulator of growth (2), and it may also directly affect protein synthesis rates. During these experiments, the EC was maintained at 0.93 ± 0.03 . In addition, the GTP concentration was maintained at approximately 1 mM, which is much greater than the system K_m^{GTP} (see below). These considerations support our conclusion that the ATP concentration controlled the rate of protein synthesis, and the observation of a Michaelis-Menten relationship for [ATP] dependence over a wide range of ATP concentrations (Fig. 4C) provides additional support.

Protein synthesis rate as a function of [GTP]. Although the ATP concentration is probably the single most important parameter influencing the entire protein synthesis system, GTP is required for translation initiation, for elongation, and for termination. To characterize the GTP dependence of the entire protein synthesis system (Fig. 1), we determined the rate of CAT accumulation at specific GTP concentrations while maintaining [ATP] at $1.0 \pm 0.1 \text{ mM}$, which was significantly greater than the system K_m^{ATP} , and while keeping the EC greater than 0.9. We observed linear CAT production with constant GTP concentrations (Fig. 5A and 5B) and again observed Michaelis-

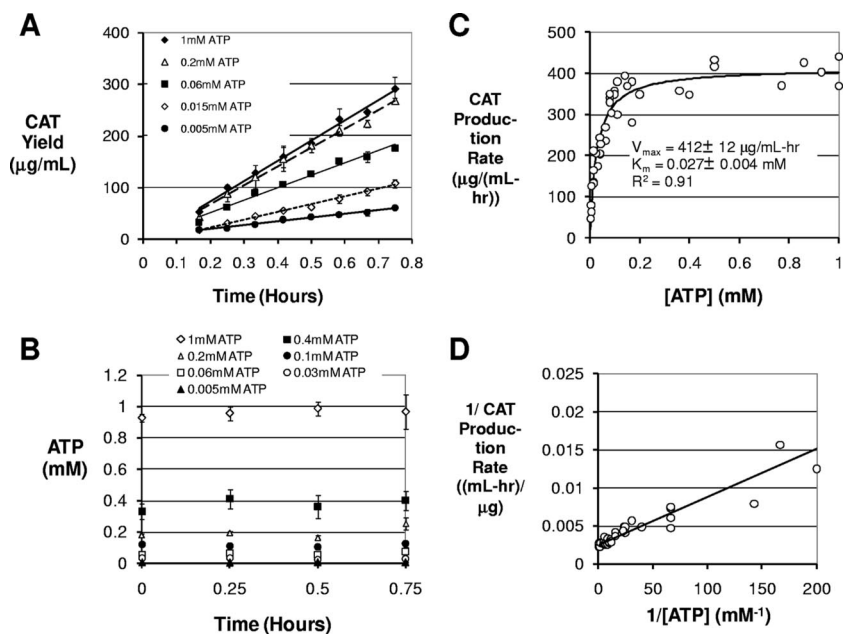


FIG. 4. Rate of protein synthesis as a function of [ATP]. (A) Representative CAT production profiles with constant ATP concentrations. The error bars indicate the ranges for two experiments. (B) Representative ATP concentration profiles during protein synthesis with constant ATP concentrations. The error bars indicate the ranges for two experiments. (C) Plot of the CAT production rate versus the substrate concentration for 37 individual experiments (\circ). (D) Lineweaver-Burk double-reciprocal plot strongly suggesting Michaelis-Menten kinetics. The data were used to determine the Michaelis constants (K_m , $27 \pm 4 \mu\text{M}$; V_{\max} , $41 \pm 1 \mu\text{g CAT/h/mg } E. coli$ protein) by a least-squares fit to the hyperbolic Michaelis-Menten equation {protein production rate = $(V_{\max} \times [\text{ATP}]) / (K_m + [\text{ATP}])$ }. The Michaelis-Menten fit is indicated by the solid line in panel C. Parameters obtained using Lineweaver-Burk linear regression analysis were consistent with the constants determined by this analysis (e.g., a K_m of $26 \mu\text{M}$). The total *E. coli* protein concentration in the reaction mixture was approximately 10 mg/ml , as determined by a Bradford assay (Bio-Rad, Hercules, CA) using bovine serum albumin as a standard.

Menten dependence (Fig. 5C and 5D). The Michaelis-Menten constants obtained by using a least-squares fit to the data in Fig. 5C are as follows: K_m^{GTP} , $14 \pm 2 \mu\text{M}$; and V_{\max} , $40 \pm 1 \mu\text{g CAT/h/mg } E. coli$ protein.

DISCUSSION

Here we determined for the first time the relationship between the ATP concentration and protein synthesis rates (K_m^{ATP} , $27 \pm 4 \mu\text{M}$). We also determined the relationship between the GTP concentration and protein synthesis rates (K_m^{GTP} , $14 \pm 2 \mu\text{M}$). To evaluate our approach, we compared our results with previous measurements obtained by using purified individual components. The system-level GTP affinity that we determined, $\sim 14 \mu\text{M}$, agrees well with the individually measured affinities of the four GTP binding proteins known to catalyze bacterial protein synthesis (IF-2 [1], EF-Tu [15], EF-G [25], and RF-3 [54]) (Table 2). This agreement provides confidence in the overall experimental system.

The system-level K_m^{ATP} , however, was unexpectedly low. Charging tRNAs with amino acids is the single most energy-demanding step in protein synthesis (44), particularly when the fact that each mRNA is used multiple times is considered (27). Therefore, we anticipated that the overall dependence of the rate on the ATP concentration might be controlled by the lowest ATP affinity reported for the aminoacyl-tRNA synthetases, which is on the order of $500 \mu\text{M}$ (17). In contrast, the protein synthesis system exhibits much stronger ATP affinity (Table 2). It is interesting that at an ATP concentration of 27

μM , such a synthetase would be expected to function at a rate that is only about 3% of the rate observed with the cytoplasmic ATP concentration present when the organism has an adequate energy source (3 mM). With $27 \mu\text{M}$ ATP the protein synthesis rate would still be 50% of the prestarvation rate.

There may be multiple reasons for the inconsistency between the system-level K_m^{ATP} and the individually measured ATP affinities for the aminoacyl-tRNA synthetases. One very probable reason is that the Cytomim system more faithfully reflects the intracellular environment than the systems used in previous studies. This includes both the activation of integrated metabolic systems, such as central metabolism, oxidative phosphorylation, mRNA turnover, and nucleotide metabolism, and reproduction of the cytoplasmic physicochemical environment (21, 22). For example, the Cytomim system includes glutamate at intracellular concentrations. Glutamate apparently acts as a buffering agent that allows the free Mg^{2+} concentration to be maintained more consistently even during periods when there is extracellular magnesium exhaustion. In our experiments (Fig. 3), more magnesium was required to obtain the maximal protein synthesis rates than was expected based on the increase in [ATP]. Undoubtedly, some of the additional Mg^{2+} complexed with glutamate, and therefore more total Mg^{2+} was required to obtain the necessary unassociated Mg^{2+} . Beyond more closely emulating the true biological effect of magnesium buffering agents, the Cytomim platform also does not include chloride (20), which can significantly perturb ionic interactions (38), or nonnatural agents,

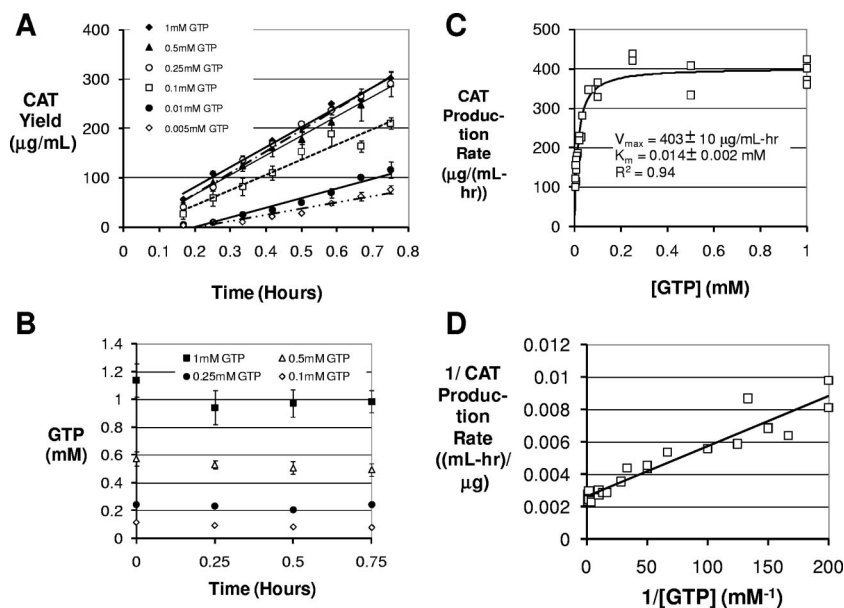


FIG. 5. Rate of protein synthesis as a function of [GTP]. (A) Representative CAT production profiles with constant GTP concentrations. The error bars indicate the ranges for two experiments. (B) Representative GTP concentration profiles for protein synthesis reactions performed with constant GTP concentrations. The error bars indicate the ranges for two experiments. (C) Plot of reaction velocity versus substrate concentration for 23 individual experiments (\square). (D) Lineweaver-Burk double-reciprocal plot strongly suggesting Michaelis-Menten kinetics. The data were used to determine the constants (K_m , $14 \pm 2 \mu\text{M}$; V_{\max} , $40 \pm 1 \mu\text{g CAT/h/mg } E. coli$ protein) by a least-squares fit to the hyperbolic Michaelis-Menten equation. The Michaelis-Menten equation fit is indicated by the solid line in panel C. Parameters obtained using Lineweaver-Burk linear regression analysis were consistent with the constants determined by this analysis (e.g., a K_m of $12 \mu\text{M}$).

such as polyethylene glycol and HEPES buffer (22, 23). Although studying the biochemical parameters of individual enzymes is extremely important, our results suggest that in some situations an integrated system may be required to accurately reflect the functional characteristics of complex multicomponent systems.

Despite our attempt to mimic the cytoplasm, three aspects of the chemical environment remain nonphysiological. First, 2.4 mM Tris is carried over into the cell-free system as a result

TABLE 2. Comparison of system-level and individual-factor GTP and ATP affinities^a

Reaction	K_m^{GTP} (μM)	K_m^{ATP} (μM)
Protein synthesis ^b	14	27
IF-2 activation	2	
EF-Tu recycling	10	
EF-G activation	10	
RF-3 activation	2.5	
Tyrosyl-tRNA acylation		4
Methionyl-tRNA acylation		430
Seranyl-tRNA acylation		100
Leucyl-tRNA acylation		130–720
Tryptophanyl-tRNA acylation		300

^a The overall system dependence on [GTP] agrees well with the individually measured affinities of the four GTP binding proteins known to catalyze bacterial protein synthesis (IF-2, EF-Tu, EF-G, and RF-3). However, the overall system dependence on [ATP] is inconsistent with the individually measured affinities of aminoacyl-tRNA synthetases (which catalyze the most energy-demanding steps of protein synthesis). For references see the text. The K_m^{ATP} s for tRNA acylation reactions are representative (for a more complete list, see references 3 and 17).

^b Data for protein synthesis are from the cell-free experiments described in this communication.

of extract preparation, adding a mild detergent. To date, our efforts to mimic the cytoplasm have focused on mimicking salts added directly to the cell-free protein synthesis system (22) without attempting to change the extract preparation procedure. Workers in our laboratory are now trying to develop new extract preparation protocols to target removal of Tris and to use glutamate salts rather than acetate salts in extract preparation. Second, 33 mM sodium is added to the reaction mixture as the cationic species complexed to pyruvate, introducing an extra parameter. We attempted to avoid the use of sodium pyruvate by using 33 mM pyruvic acid and adjusting the pH to 7.0 with potassium hydroxide or ammonium hydroxide. Unfortunately, the protein synthesis rates and yields decreased significantly under these conditions for unknown reasons. Recently, however, we discovered that the Cytomim system can be fueled by glutamate salts alone (21). Using the pyruvate-free system could eliminate any possible effects of sodium on the system. The third nonphysiological aspect of the system is that phosphate concentrations are low. In the experimental apparatus used here, the lower and upper bounds of the phosphate concentration in the reaction mixture are between 0.5 and 5 mM (22). Increasing the phosphate concentration may help activate phosphorylation reactions (e.g., nucleotide regeneration and metabolism) and phosphorolysis (13). As shown in Fig. 1, nucleotide regeneration, phosphorolysis (where inorganic phosphate attacks mRNA), and mRNA degradation by RNases are important components of nucleotide metabolism that provide coupling between transcription, protein synthesis, and mRNA turnover (13, 37). Nucleotide metabolism is also relevant in central metabolism (e.g., in the regulation of glycolysis [10]) and in DNA synthesis, although these processes

are not shown in Fig. 1. Adding higher concentrations of phosphate to the cell-free system may encourage more natural metabolism. For example, we recently showed that supplementing the pyruvate-free Cytomim system with 10 mM phosphate (the optimum experimental concentration) increased protein synthesis yields (21). On the other hand, the low phosphate concentrations used here may have restricted ATP regeneration inside the reaction chamber and therefore may have been necessary to maintain low ATP concentrations. More closely emulating the cytoplasmic environment by addressing these three aspects of the chemical environment is expected to encourage more natural behavior and may impact our results. We believe that deviations caused by insufficient reproduction of *in vivo* conditions likely would have resulted in a K_m^{ATP} higher than the true value. Thus, at a minimum, our data provide a conservative estimate of the K_m^{ATP} for protein synthesis.

While the low K_m^{ATP} was unexpected if aminoacylation was rate limiting, another possibility is that while aminoacylation is the most energy-intensive step, it is not the limiting step. If elongation, for example, were the rate-limiting step under energy-limited conditions, then the rate of aminoacylation may be far lower than the maximum rate and still provide ample aminoacyl-tRNA for protein synthesis. Because tRNAs from a commercial source are added to the cell-free system, there are excess tRNAs relative to other translational components. This is consistent with the interpretation that surplus aminoacyl-tRNAs could accumulate if elongation was limiting. However, we observed that a lack of tRNA addition had a very minor effect on cell-free protein synthesis, decreasing yields by at most 5%. An interesting follow-up study might be to use a cell-free translation system reconstituted from purified elements (41). Here, the levels of tRNAs could be fine-tuned without endogenous background levels. tRNA levels could be decreased, if necessary, until they were rate limiting, and the K_m^{ATP} could be determined.

Regardless of the reason for the unexpectedly low K_m^{ATP} , the high ATP affinity has important implications for how cells can remodel themselves when they are energy starved. While high ATP affinity is most likely a general phenomenon, we constrained interpretation of our results to the case where cells are shifted from rapid growth to energy-limited conditions. There are two reasons for this. First, the extract source cells were grown in a nutrient-rich environment. Second, the dilute conditions of the cell-free system (~20-fold less concentrated than *in vivo*) are characteristic of the lower growth rates that would result from energy limitation. Rapidly growing cells (growth rate, 1.7 h^{-1}) contain ~73,000 ribosomes per cell (5). With lower growth rates, the ribosome concentrations decrease and approach concentrations similar to those in our cell-free reactions. For example, the number of ribosomes per cell decreases ~10-fold when the growth rate is 0.4 h^{-1} (5). It is expected that other factors required for translation are coordinately regulated. Thus, the concentrations in the cell-free system tend to mimic the intracellular concentrations of translational components during periods of slow growth.

In contrast to growth in the laboratory, bacterial growth in the wild is more accurately characterized by feast or famine (28). In one study of stationary-phase metabolism, where the reason for entry into stationary phase was not precisely deter-

mined, the ATP concentration decreased to about 25% of the concentration during active growth (29). Under conditions in which there is prolonged energy starvation, the ATP levels almost certainly become much lower than this, but bacteria still need to replace catalysts that become inactive and to produce new catalysts in order to effectively adapt (28). It is likely that the intracellular glutamate stores can be used as an emergency fuel supply, as indicated by the results of cell-free studies with radiolabeled glutamate (21). Nonetheless, ATP must be used frugally to allow the often significant remodeling of the cell required for stationary-phase survival. The high affinity of protein synthesis for ATP suggests that cells can ration ATP based on the ATP affinities of the competing energy-dependent processes and still make significant quantities of new protein. This would provide a crucial survival advantage when cells are shifted from rapid-growth conditions to energy-limited conditions.

It has been reported that other ATP-dependent cellular systems and enzymes central to survival have high ATP affinities. For example, ATP-dependent proteases are essential for the breakdown of intracellular proteins during starvation both to stop undesirable reactions and to provide amino acids for new protein synthesis (33, 43). The ATP-dependent protease Lon is the major enzyme involved in proteolytic degradation in *E. coli*. The affinity of Lon for ATP (K_m^{ATP} , $7.8 \mu\text{M}$) (9), is on the order of the affinity observed for protein synthesis. Ion-transporting ATPases, which provide an important transmembrane electrochemical gradient and modify the cytoplasmic pH under stress conditions, are another example (49, 50). It is likely that ATP rationing among such essential, energy-dependent metabolic processes provides an important survival advantage and is enforced by the relative ATP affinities.

Since cell-free protein synthesis is emerging as a potential commercial recombinant DNA protein expression technology (24, 45, 51), it is also interesting that the modern systems do not appear to be energy limited. The measured ATP and GTP concentrations ($200 \mu\text{M}$ or higher) are much higher than the $K_m\text{s}$ for protein synthesis (21, 22, 23).

We used a prokaryotic combined transcription-translation system to show, for the first time, the relationship between protein synthesis rate and ATP concentration. We observed that the protein synthesis system exhibits much stronger ATP affinity than the ATP affinity suggested by characterization of individual enzymes. We also determined the dependence of protein synthesis rate on [GTP], which agrees with previous data for *in vitro* enzyme measurements and provides confidence in our data. The high affinity of the protein synthesis system for ATP and GTP underscores the ability of cells to remodel themselves upon a shift from high growth rates to energy-limited conditions. Moreover, this work demonstrates the importance of using cell-free biology as an integrated platform to obtain accurate information about the behavior of metabolic systems in which there are complex and often poorly understood interactions. We expect that this analytical approach will open the door for testing many hypotheses that deepen our understanding of the mechanisms controlling metabolic systems. For example, the same experimental system can be used to explore the effects of EC while a constant ATP concentration is maintained.

ACKNOWLEDGMENTS

We thank Joseph D. Puglisi, Chaitan Khosla, and Dan Fraenkel for critical discussions and for reading the manuscript.

This work was supported by grant ROI-GM60615 from the NIH to J.R.S. M.C.J. was also supported by a predoctoral fellowship from the Stanford NIH training program in biotechnology. M.C.J. and J.R.S. designed the study. M.C.J., M.L.M., and Y.C. carried out the experiments. M.C.J. analyzed the data. M.C.J. and J.R.S. wrote the manuscript. All authors discussed data and commented on the manuscript.

REFERENCES

1. Antoun, A., M. Y. Pavlov, K. Andersson, T. Tenson, and M. Ehrenberg. 2003. The roles of initiation factor 2 and guanosine triphosphate in initiation of protein synthesis. *EMBO J.* **22**:5593–5601.
2. Atkinson, D. E. 1968. The energy charge of the adenylate pool as a regulatory parameter. Interaction with feedback modifiers. *Biochemistry* **7**:4030–4034.
3. Bergmann, F. H., P. Berg, and M. Dieckmann. 1961. The enzymatic synthesis of amino acyl derivatives of ribonucleic acid. II. The preparation of leucyl-, valyl-, isoleucyl-, and methionyl ribonucleic acid synthetases from *Escherichia coli*. *J. Biol. Chem.* **236**:1735–1740.
4. Blanchard, S. C., R. L. Gonzalez, Jr., H. D. Kim, S. Chu, and J. D. Puglisi. 2004. tRNA selection and kinetic proofreading in translation. *Nat. Struct. Mol. Biol.* **11**:1008–1014.
5. Bremer, H., and P. P. Dennis. 1996. Modulation of chemical composition and other parameters of the cell by growth rate, p. 1553–1569. *In* F. C. Neidhardt, R. Curtiss III, J. L. Ingraham, E. C. C. Lin, K. B. Low, B. Magasanik, W. S. Reznikoff, M. Riley, M. Schaechter, and H. E. Umbarger (ed.), *Escherichia coli* and *Salmonella*: cellular and molecular biology, 2nd ed. American Society for Microbiology, Washington, DC.
6. Calhoun, K. A., and J. R. Swartz. 2005. Energizing cell-free protein synthesis with glucose metabolism. *Biotechnol. Bioeng.* **90**:606–613.
7. Calhoun, K. A., and J. R. Swartz. 2006. Total amino acid stabilization during cell-free protein synthesis reactions. *J. Biotechnol.* **123**:193–203.
8. Chapman, A. G., L. Fall, and D. E. Atkinson. 1971. Adenylate energy charge in *Escherichia coli* during growth and starvation. *J. Bacteriol.* **108**:1072–1086.
9. Chung, C. H., and A. L. Goldberg. 1981. The product of the lon (capR) gene in *Escherichia coli* is the ATP-dependent protease, protease La. *Proc. Natl. Acad. Sci. USA* **78**:4931–4935.
10. Danchin, A., L. Dondon, and J. Daniel. 1984. Metabolic alterations mediated by 2-ketobutyrate in *Escherichia coli*-K12. *Mol. Gen. Genet.* **193**:473–478.
11. Dawson, R. M. C., D. C. Elliott, W. H. Elliott, and K. M. Jones. 1990. Data for biochemical research. Oxford University Press, New York, NY.
12. Dinbier, U., E. Limpinsel, R. Schmid, and E. P. Bakker. 1988. Transient accumulation of potassium glutamate and its replacement by trehalose during adaptation of growing cells of *Escherichia coli* K-12 to elevated sodium chloride concentrations. *Arch. Microbiol.* **150**:348–357.
13. Donovan, W. P., and S. R. Kushner. 1986. Polynucleotide phosphorylase and ribonuclease II are required for cell viability and mRNA turnover in *Escherichia coli* K-12. *Proc. Natl. Acad. Sci. USA* **83**:120–124.
14. Fenton, W. A., and A. L. Horwich. 1997. GroEL-mediated protein folding. *Protein Sci.* **6**:743–760.
15. Gromadski, K. B., H. J. Wieden, and M. V. Rodnina. 2002. Kinetic mechanism of elongation factor Ts-catalyzed nucleotide exchange in elongation factor Tu. *Biochemistry* **41**:162–169.
16. Hartl, F. U. 1996. Molecular chaperones in cellular protein folding. *Nature* **381**:571–580.
17. Hershey, J. W. B. 1987. Protein synthesis, p. 613–647. *In* F. C. Neidhardt, J. L. Ingraham, K. B. Low, B. Magasanik, M. Schaechter, and H. E. Umbarger (ed.), *Escherichia coli* and *Salmonella*: cellular and molecular biology, 1st ed. American Society for Microbiology, Washington, DC.
18. Hopfield, J. J. 1974. Kinetic proofreading: a new mechanism for reducing errors in biosynthetic processes requiring high specificity. *Proc. Natl. Acad. Sci. USA* **71**:4135–4139.
19. Ishii, N., K. Nakahigashi, T. Baba, M. Robert, T. Soga, A. Kanai, T. Hirasawa, M. Naba, K. Hirai, A. Hoque, P. Y. Ho, Y. Kakazu, K. Sugawara, S. Igarashi, S. Harada, T. Masuda, N. Sugiyama, T. Togashi, M. Hasegawa, Y. Takai, K. Yugi, K. Arakawa, N. Iwata, Y. Toya, Y. Nakayama, T. Nishioka, K. Shimizu, H. Mori, and M. Tomita. 2007. Multiple high-throughput analyses monitor the response of *E. coli* to perturbations. *Science* **316**:593–597.
20. Jelenc, P. C., and C. G. Kurland. 1979. Nucleoside triphosphate regeneration decreases the frequency of translation errors. *Proc. Natl. Acad. Sci. USA* **76**:3174–3178.
21. Jewett, M. C., K. A. Calhoun, A. Voloshin, J. J. Wu, and J. R. Swartz. 2008. An integrated cell-free metabolic platform for protein production and synthetic biology. *Mol. Syst. Biol.* **4**:220.
22. Jewett, M. C., and J. R. Swartz. 2004. Mimicking the *Escherichia coli* cytoplasmic environment activates long-lived and efficient cell-free protein synthesis. *Biotechnol. Bioeng.* **86**:19–26.
23. Jewett, M. C., and J. R. Swartz. 2004. Substrate replenishment extends protein synthesis with an in vitro translation system designed to mimic the cytoplasm. *Biotechnol. Bioeng.* **87**:465–472.
24. Kanter, G., J. Yang, A. Voloshin, S. Levy, J. R. Swartz, and R. Levy. 2007. Cell-free production of scFv fusion proteins: an efficient approach for personalized lymphoma vaccines. *Blood* **109**:3393–3399.
25. Katunin, V. I., A. Savelsbergh, M. V. Rodnina, and W. Wintermeyer. 2002. Coupling of GTP hydrolysis by elongation factor G to translocation and factor recycling on the ribosome. *Biochemistry* **41**:12806–12812.
26. Kim, D. M., and C. Y. Choi. 1996. A semi-continuous prokaryotic coupled transcription/translation system using a dialysis membrane. *Biotechnol. Prog.* **12**:645–649.
27. Kim, D. M., and J. R. Swartz. 2001. Regeneration of adenosine triphosphate from glycolytic intermediates for cell-free protein synthesis. *Biotechnol. Bioeng.* **74**:309–316.
28. Kolter, R., D. A. Siegle, and A. Tormo. 1993. The stationary phase of the bacterial life cycle. *Annu. Rev. Microbiol.* **47**:855–874.
29. Murray, H. D., D. A. Schneider, and R. L. Gourse. 2003. Control of rRNA expression by small molecules is dynamic and nonredundant. *Mol. Cell* **12**:125–134.
30. Neijssel, O. M., M. J. Teixeira de Mattos, and D. W. Tempest. 1996. Growth yield and energy distribution, p. 1683–1692. *In* F. C. Neidhardt, R. Curtiss III, J. L. Ingraham, E. C. C. Lin, K. B. Low, B. Magasanik, W. S. Reznikoff, M. Riley, M. Schaechter, and H. E. Umbarger (ed.), *Escherichia coli* and *Salmonella*: cellular and molecular biology, 2nd ed. American Society for Microbiology, Washington, DC.
31. Neuhard, J., and P. Nygaard. 1987. Purines and pyrimidines, p. 445–473. *In* F. C. Neidhardt, J. L. Ingraham, K. B. Low, B. Magasanik, M. Schaechter, and H. E. Umbarger (ed.), *Escherichia coli* and *Salmonella*: cellular and molecular biology, 1st ed. American Society for Microbiology, Washington, DC.
32. Ohashi, Y., A. Hirayama, T. Ishikawa, S. Nakamura, K. Shimizu, Y. Ueno, M. Tomita, and T. Soga. 2008. Depiction of metabolome changes in histidine-starved *Escherichia coli* by CE-TOFMS. *Mol. Biosyst.* **4**:135–147.
33. Olden, K., and A. L. Goldberg. 1978. Studies of the energy requirement for intracellular protein degradation in *Escherichia coli*. *Biochim. Biophys. Acta* **542**:385–398.
34. Pavlov, M. Y., and M. Ehrenberg. 1996. Rate of translation of natural mRNAs in an optimized in vitro system. *Arch. Biochem. Biophys.* **328**:9–16.
35. Petersen, C., and L. B. Moller. 2000. Invariance of the nucleoside triphosphate pools of *Escherichia coli* with growth rate. *J. Biol. Chem.* **275**:3931–3935.
36. Py, B., C. F. Higgins, H. M. Krisch, and A. J. Carpousis. 1996. A DEAD-box RNA helicase in the *Escherichia coli* RNA degradosome. *Nature* **381**:169–172.
37. Rauhut, R., and G. Klug. 1999. mRNA degradation in bacteria. *FEMS Microbiol. Rev.* **23**:353–370.
38. Record, M. T., Jr., E. S. Courtenay, S. Cayley, and H. J. Guttman. 1998. Biophysical compensation mechanisms buffering *E. coli* protein-nucleic acid interactions against changing environments. *Trends Biochem. Sci.* **23**:190–194.
39. Record, M. T., Jr., E. S. Courtenay, S. Cayley, and H. J. Guttman. 1998. Responses of *E. coli* to osmotic stress: large changes in amounts of cytoplasmic solutes and water. *Trends Biochem. Sci.* **23**:143–148.
40. Schneider, D. A., and R. L. Gourse. 2004. Relationship between growth rate and ATP concentration in *Escherichia coli*: a bioassay for available cellular ATP. *J. Biol. Chem.* **279**:8262–8268.
41. Shimizu, Y., T. Kanamori, and T. Ueda. 2005. Protein synthesis by pure translation systems. *Methods* **36**:299–304.
42. Snoep, J. L., F. Bruggeman, B. G. Olivier, and H. V. Westerhoff. 2006. Towards building the silicon cell: a modular approach. *Biosystems* **83**:207–216.
43. St. John, A. C., and A. L. Goldberg. 1978. Effects of reduced energy production on protein degradation, guanosine tetraphosphate, and RNA synthesis in *Escherichia coli*. *J. Biol. Chem.* **253**:2705–2711.
44. Stryer, L. 1995. *Biochemistry*, 4th ed. W. H. Freeman and Company, New York, NY.
45. Swartz, J. R. 2006. Developing cell-free biology for industrial applications. *J. Ind. Microbiol. Biotechnol.* **33**:476–485.
46. Swartz, J. R., M. C. Jewett, and K. Woodrow. 2004. Cell-free protein synthesis with prokaryotic coupled transcription-translation, p. 169–182. *In* P. Balbas and A. Lorence (ed.), *Recombinant protein protocols*. Methods in Molecular Biology Series. Humana Press, Totowa, NJ.
47. Underwood, K. A., J. R. Swartz, and J. D. Puglisi. 2005. Quantitative polysome analysis identifies limitations in bacterial cell-free protein synthesis. *Biotechnol. Bioeng.* **91**:425–435.
48. Wacker, W. E. 1969. The biochemistry of magnesium. *Ann. N. Y. Acad. Sci.* **162**:717–726.
49. Weber, J., S. Wilke-Mounts, R. S. Lee, E. Grell, and A. E. Senior. 1993. Specific placement of tryptophan in the catalytic sites of *Escherichia coli* F1-ATPase provides a direct probe of nucleotide binding: maximal ATP hydrolysis occurs with three sites occupied. *J. Biol. Chem.* **268**:20126–20133.
50. Weber, J., S. Wilke-Mounts, and A. E. Senior. 1994. Cooperativity and stoichiometry of substrate binding to the catalytic sites of *Escherichia coli*

- F1-ATPase. Effects of magnesium, inhibitors, and mutation. *J. Biol. Chem.* **269**:20462–20467.
51. **Yang, J., G. Kanter, A. Voloshin, N. Michel-Reydellet, H. Velkeen, R. Levy, and J. R. Swartz.** 2005. Rapid expression of vaccine proteins for B-cell lymphoma in a cell-free system. *Biotechnol. Bioeng.* **89**:503–511.
52. **Yao, S. L., X. C. Shen, and E. Suzuki.** 1997. Biochemical energy consumption by wheat germ extract during cell-free protein synthesis. *J. Ferment. Bioeng.* **84**:7–13.
53. **Zavialov, A. V., and M. Ehrenberg.** 2003. Peptidyl-tRNA regulates the GTPase activity of translation factors. *Cell* **114**:113–122.
54. **Zavialov, A. V., R. H. Buckingham, and M. Ehrenberg.** 2001. A posttermination ribosomal complex is the guanine nucleotide exchange factor for peptide release factor RF3. *Cell* **107**:115–124.
55. **Zawada, J. F., B. Richter, E. Huang, E. Loades, A. Shah, and J. R. Swartz.** 2003. High density, defined media culture for production of *Escherichia coli* extracts. *Ferment. Biotechnol.* **862**:142–156.